Journal of Computational Physics **148,** 497–526 (1999)
Article ID jcph.1998.6127, available online at http://www.idealibrary.com on IDEAL®

Improved Treatment of Source Terms in Upwind Schemes for the Shallow Water Equations in Channels with Irregular Geometry

María Elena Vázquez-Cendón

Departamento de Matemática Aplicada, Universidade de Santiago, 15706 Santiago de Compostela, Spain
E-mail: elena@zmat.usc.es

Received March 25, 1998; revised September 28, 1998

This paper deals with the numerical solution of the shallow water equations in channels with irregular geometry but with a locally rectangular cross section. This type of channel leads to the presence of source terms involving the gradient of the depth and the breadth of the channel. Extensions of the Q-scheme of van Leer and Roe are proposed which generate natural upwind discretizations of the source terms. The consistency of the proposed schemes is analyzed. A stationary solution that emphasizes the source terms considered is obtained which is used to test the proposed extensions in terms of a "conservation" property. A low-order asymptotic unsteady analytical solution for a small Froude number is also obtained. The numerical results presented confirm the improved properties of the proposed schemes for a transient test problem.

Key Words: upwind schemes; source terms; shallow water equations; channels with irregular geometry.

1. INTRODUCTION

Numerical solutions of hydrodynamic problems offer the possibility of predicting the behaviour of the relevant variables in practical situations. In particular, the one-dimensional shallow water equations can be solved in order to determine the flow variables in channels.

In these equations, the channel or river geometry, characterized by the bed depth and cross section functions, has a special relevance. For channels with variable bed and rectangular cross section there are source terms involving the bed slope, as well as the breadth function and its derivative; moreover, consideration of bottom friction leads to an additional source term.

The hyperbolic system of homogeneous shallow water equations can be written in conservative form and the presence of source terms leads to the mathematical framework of

0021-9991/99 $30.00

a numerical solution of hyperbolic systems of conservation laws with source terms (see LeVeque [13], Godlewski and Raviart [8], and Toro [20]).

Although upwind schemes were initially developed for the Euler equations, in recent years the number of papers devoted to the numerical solution of the shallow water equations with Riemann solvers has increased (see Glaister [6], Alcrudo and García Navarro [1]). The discretization of the source terms has been studied by a large number of authors (see, e.g., [19, 7, 17, 14, 10]).

In previous papers (Bermúdez and Vázquez [3], for the one-dimensional case, and Bermúdez, Dervieux, Desideri, and Vázquez [2], in the two-dimensional case) the importance of upwinding the source term involving the bed slope in channels with constant breadth has been proved. In this paper, in order to motivate the advantage of upwinding the more general source terms, we start by showing the unsatisfactory results obtained when using centred discretizations in a stationary problem. These results are compared with the corresponding exact stationary solution also obtained in the present paper. This solution will be referenced when we study the conservation of the schemes. An upwind discretization for these source terms is also proposed. In some sense, the source terms are upwinded in a similar way to the numerical flux, although there are different expressions for each method. We generalize for nonuniform meshes the Q-schemes of van Leer and Roe with tools introduced in Bermúdez and Vázquez [3] to nonhomogeneous problems. This generalization is very important in order to use the adaptive mesh techniques to reduce the number of nodes and to improve the accuracy.

The consistency and conservation of the proposed schemes for nonuniform meshes are analyzed from the theoretical point of view. Let us notice that the two upwind schemes considered here are conservative for homogeneous problems. Nevertheless, the conservation of the extended schemes must be proved in the presence of source terms.

As in [3], the introduction of the conservation property is connected with steady solutions. More particularly, a numerical scheme applied to the shallow water equations is termed conservative if it approximates, exactly or with order greater than one, a stationary solution when including the different source terms studied. It is proved that these extensions verify this property, and the new steady solution is present this study.

In addition to the theoretical analysis of the properties of the proposed schemes, numerical results are shown. In order to illustrate the improved performance of the new extensions, the results are compared not only with the mentioned stationary solution associated with the conservation property but also with an "asymptotic" unsteady solution that is also obtained in this paper.

It is worth noting at this point that the analytical solutions presented in the literature correspond to either constant depth and variable breadth or constant breadth and variable depth (see MacDonald [16]). An important contribution of this work comes from the possibility of analyzing the joint behaviour of both source terms by means of the asymptotic solution obtained here, which includes variable depth and breadth and also bottom friction effects. In order to deduce this solution it is convenient to write the equations in dimensionless form so that the solution is obtained by means of asymptotic expansions in terms of the Froude number. The solution is valid for small values of this parameter and when the domain is "small."

The improved properties of the proposed schemes are also shown in problems presented in the literature: the flow over a bump in critical situations (see [9]) and two test problems described by García-Navarro *et al.* [4]; a steady flow (with a hydraulic jump) and a

surge propagation (a transitory motion with supercritical situations), both in a converging–diverging channel with constant depth.

The shallow water equations are stated in Section 2. The numerical discretization is presented in Section 3, where the general class of upwind methods for nonhomogeneous conservation laws introduced in Bermúdez and Vázquez [3] is generalized to nonuniform meshes and applied to the source terms. For the shallow water equations these schemes are also compared with a "conservation property related to a stationary solution" in Section 4. Finally, in Section 5, numerical results are shown and compared with those obtained using centred discretizations of the source terms and with the "analytical" solution for the tidal propagation test and also for the mentioned classical problems. Finally, the conclusions are presented.

2. SHALLOW WATER EQUATIONS FOR THE CHANNELS WITH RECTANGULAR CROSS SECTION

The one-dimensional flow in an open channel of variable breadth and depth, but with a locally rectangular cross section, may be described by the Saint-Venant equations which are written in conservative form as

$$\frac{\partial \tilde{W}}{\partial t}(x,t) + \frac{\partial \tilde{F}}{\partial x}(\tilde{W}(x,t)) = \tilde{G}(x,\tilde{W}(x,t)), \tag{1}$$

$$\tilde{W} = \begin{pmatrix} S \\ Su \end{pmatrix} = \begin{pmatrix} S \\ Q \end{pmatrix}, \quad \tilde{F}(\tilde{W}) = \begin{pmatrix} Q \\ \frac{Q^2}{S} \end{pmatrix} \tag{2}$$

$$\tilde{G}(x,\tilde{W}) = \begin{pmatrix} 0 \\ -gS\left(\frac{\partial h}{\partial x} - H'(x)\right) - \frac{gQ|Q|\mathrm{M}^2}{SR_h^{4/3}} \end{pmatrix} \tag{3}$$

(see Fig. 1).

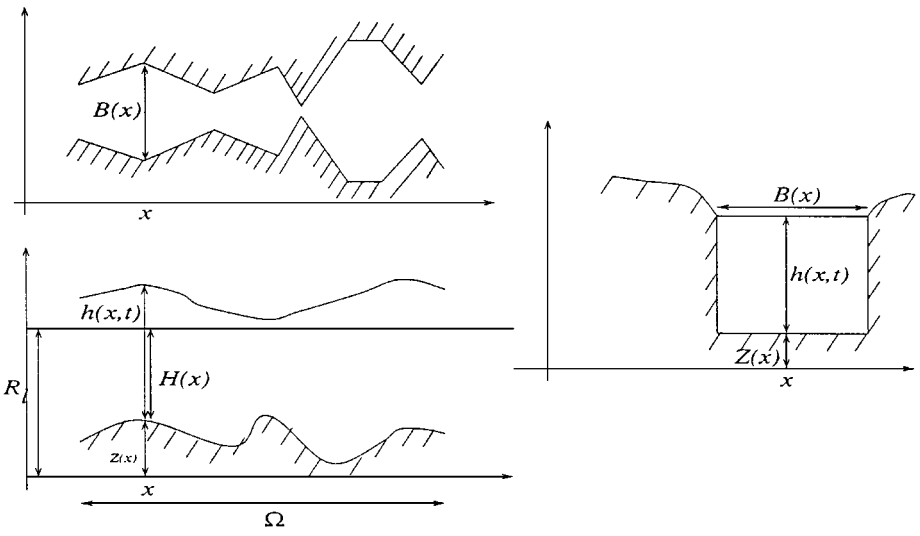

FIG. 1. Shallow domain.

The two components of the conservative variable $\tilde{W}$ represent the cross-section area $S = S(x, t)$ and the massflow $Q = Q(x, t) = Su$, and u and h denote the average horizontal velocity and the total height above the bottom of the channel, at position x and time t, respectively. The hydraulic radius is denoted by R_h, M is the Manning coefficient, $Z = Z(x)$ is the bottom function, and $H(x)$ the depth of the same point but from a fixed reference level $R_l = Z(x) + H(x)$. $\Omega = [0, L]$ denotes the projection of the domain occupied by the fluid onto the X axis.

We consider a locally rectangular channel, so that

$$S(x, t) = B(x)h(x, t), \tag{4}$$

where $B(x)$ is the breadth of the channel.

Replacing the expression S of (4) in Eq. (1) we obtain a new form of the equations with new unknowns. The components of the new unknown, called w, are the height of the fluid h and $q = hu$. Let us observe that these are the same as in the one-dimensional shallow water equations for channels with constant breadth (i.e., when $B(x) = 1\ \forall x \in \Omega$).

$$\frac{\partial w}{\partial t}(x, t) + \frac{\partial F}{\partial x}(w(x, t)) = \sum_{k=1}^{3} G_k(x, w(x, t)), \tag{5}$$

where

$$w = \begin{pmatrix} h \\ q \end{pmatrix}, \quad F(w) = \begin{pmatrix} q \\ \frac{q^2}{h} + \frac{1}{2}gh^2 \end{pmatrix}, \quad G_1(x, w) = \begin{pmatrix} 0 \\ ghH'(x) \end{pmatrix} \tag{6}$$

$$G_2(x, w) = \begin{pmatrix} -q\frac{B'(x)}{B(x)} \\ -\frac{q^2}{h}\frac{B'(x)}{B(x)} \end{pmatrix}, \quad G_3(x, w) = \begin{pmatrix} 0 \\ -M^2 gq\left|\frac{q}{h}\right|(R_h)^{-4/3} \end{pmatrix}. \tag{7}$$

The reason why three source terms have been distinguished is to allow them to be discretized in separate ways. The source term G_1 includes the bed slope, G_2 contains the breadth variation, and finally G_3 models the bottom friction.

The boundary conditions will be introduced as

$$h(0, t) = \varphi(t) + H(0) \tag{8}$$

$$q(L, t) = \psi(t), \tag{9}$$

where $\varphi(t)$ and $\psi(t)$ will be given functions.

3. NUMERICAL DISCRETIZATION

An explicit time discretization is used, together with a finite volume method with upwinding to discretize in space. Starting from an approximation W^n of the exact solution $w(\cdot, t_n)$ and using the explicit Euler scheme, we obtain

$$\frac{W^{n+1}(x) - W^n(x)}{\Delta t} + \frac{\partial F}{\partial x}(W^n(x)) = \sum_{k=1}^{3} G_k(x, W^n). \tag{10}$$

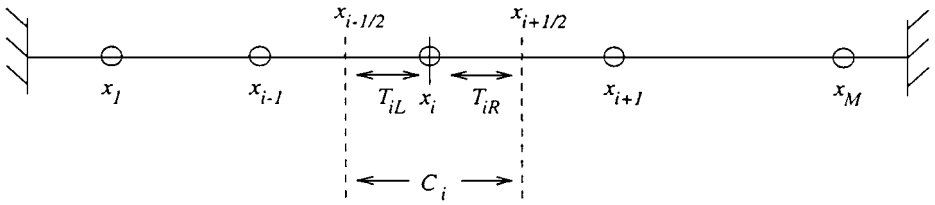

FIG. 2. Cell C_i.

The spatial domain is discretized by taking an arbitrary mesh $\mathcal{C}_{\Delta x}$. Let $\{x_i : i \in \mathbb{Z}\}$ be the nodes of $\mathcal{C}_{\Delta x}$, where Δx denotes the norm

$$\Delta x = \sup_{x_i \in \mathcal{C}_{\Delta x}} |x_i - x_{i-1}| \tag{11}$$

of $\mathcal{C}_{\Delta x}$. The cell C_i is defined as (see Fig. 2)

$$C_i = (x_{i-1/2}, x_{i+1/2}) = \left(x_i - \frac{x_i - x_{i-1}}{2}, x_i + \frac{x_{i+1} - x_i}{2}\right),$$

so that its length is given by $A_i = (x_{i+1} - x_{i-1})/2$.

The approximate solution W^n to w at t_n is considered as a piecewise constant function given by

$$W^n(x) = W_i^n \quad \text{for } x \in C_i.$$

To obtain the spatial approximation of (1), we integrate (10) over the cell C_i. This leads to the explicit scheme

$$\frac{W_i^{n+1} - W_i^n}{\Delta t} + \frac{F_{i+1/2}^n - F_{i-1/2}^n}{\Delta x} = \sum_{k=1}^{3} G_{ki}^n, \tag{12}$$

where $F_{i\pm1/2}^n$ and G_{ki}^n denote approximations of $F(W^n(x_{i\pm1/2}))$ and $(1/A_i)\int_{C_i} G_k(x, W^n)\,dx$, respectively.

3.1. *The Q-Schemes of Roe and van Leer*

Three-point upwind schemes can be obtained by replacing $F_{i\pm1/2}^n$ by values of a numerical flux function, ϕ. More precisely,

$$F_{i-1/2}^n = \phi\big(W_{i-1}^n, W_i^n\big), \quad F_{i+1/2}^n = \phi\big(W_i^n, W_{i+1}^n\big). \tag{13}$$

In particular, the Q-schemes are a family of three point upwind schemes corresponding to numerical fluxes of the form

$$\phi(V, W) = \frac{F(V) + F(W)}{2} - \frac{1}{2}|Q(V, W)|(W - V), \tag{14}$$

where Q is a matrix characteristic of each Q-scheme having a continuous dependence on the two states V and W. In this work we use the Q-schemes of van Leer and Roe:

- The Q-scheme of van Leer [12] corresponds to a choice of Q equal to the Jacobian matrix $\mathcal{A}$ of the flux evaluated at the arithmetic mean value of V and W:

$$Q(V, W) = \mathcal{A}\left(\frac{V + W}{2}\right). \tag{15}$$

- The Roe scheme is based on a linearization of the flux. In the case Q is a diagonalizable matrix which satisfies the property:

$$F(W) - F(V) = Q(V, W)(W - V). \tag{16}$$

There are different ways of choosing a matrix Q satisfying (16). Roe [18] proposed to define Q as the Jacobian matrix $\mathcal{A}$ evaluated at some state $\tilde{W} = \tilde{W}(V, W)$ known as the *Roe average* of V and W. In [6] Glaister gives $\tilde{W}$ for the shallow water equations.

The scheme is given by (12), (13), and (14).

3.2. *A New Stationary Solution: Analysis of Centred Discretizations of the Source Terms*

As already mentioned, if the geometry changes along the channel then G_1 and G_2 do not vanish. Moreover, if we include bed friction we also have the source term G_3.

Consider first centred discretizations of the source terms. In previous papers, [3, 2], we have proved that centred discretizations of the source term G_1, combined with flux-difference techniques for the flux term (14), are responsible for spurious numerical waves when the time discretization step is not small enough. This analysis is related to the ability of a numerical scheme to approximate, exactly or with order greater than one, the stationary solution of "water at rest" ($h \equiv H, q \equiv 0$).

In the present work a similar analysis is performed. However, the previously mentioned stationary solution (water at rest) involves $q \equiv 0$ so that G_2 and G_3 vanish and no conclusions can be drawn. Instead, we propose a new stationary solution in which the source terms G_2 and G_3 play a role in order to derive information about their discretization. For this reason u is taken as the inverse function of B and h is constant, giving

$$h(x, t) = \bar{h} \tag{17}$$

$$q(x, t) = \frac{\bar{h}k}{B(x)}, \tag{18}$$

where $\bar{h}$ and k are constants.

Consider a channel whose breadth function is known and where bottom friction is taken into account. The question is how to determine the depth function so that (17)–(18) is a solution of the shallow water equations. After some algebraic manipulation the depth function H is found to be given by

$$H(x) = H(x_I) + \frac{k^2}{2g}\left(\frac{1}{B^2(x)} - \frac{1}{B^2(x_I)}\right) + M^2 R_h^{-4/3} k|k| \int_{x_I}^{x} \frac{1}{B^2(s)}\, ds. \tag{19}$$

TABLE I
Values of Breadth Function at the Points x

x	0	50	100	150	200	250	300	350	400	425	435	450	470	475	500
$B(x)$	40	40	30	30	20	30	30	25	25	30	35	35	40	40	40
x	505	530	550	565	575	600	650	700	750	800	820	900	950	1000	1500
$B(x)$	45	45	50	45	40	40	30	40	40	5	40	35	25	40	40

As a test problem a subcritical case is chosen. Then the eigenvalues of the Jacobian matrix of the flux must satisfy

$$\lambda_1(w) = \frac{q}{h} + \sqrt{gh} > 0 \tag{20}$$

$$\lambda_2(w) = \frac{q}{h} - \sqrt{gh} < 0. \tag{21}$$

Taking the exact solution (17), (18) into account, the relations (20) and (21) imply that

$$\left| \frac{k}{\sqrt{gh}} \right| < \min_{x \in \Omega} B(x). \tag{22}$$

For the breadth function we take an irregular function in order to study the behaviour of the schemes near points of discontinuity. In particular we select the same breadth function considered by the *working group on dam break modelling* [9] to test the behaviour of the schemes for the source terms (see Fig. 3 and Table I). For this function the minimum value in (22) is 5 m. Thus two possible values of $\bar{h}$ and k are

$$\bar{h} = 1 \text{ m}, \quad k = 10. \tag{23}$$

In order to perform an independent analysis of the source terms G_2 and G_3, we begin by assuming that $M \equiv 0$ so as to be able to consider only G_2.

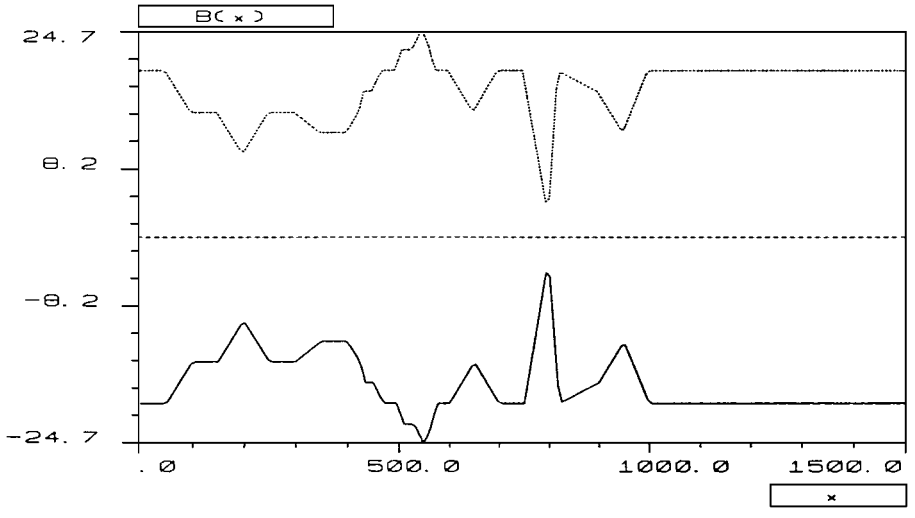

FIG. 3. Breadth of the channel.

It is important to notice that in this case the Q matrix is the same for both the Roe and van Leer Q-schemes. Therefore the numerical results we need to consider only one of them. The upwind discretization proposed in [3] is used for G_1 for the Q-scheme of van Leer, and a centred scheme is applied to the source term G_2. In order to examine this choice the discretizations are detailed. It is considered that at time $t = t_n$ the approximated solution and the exact solution are equal:

$$h_i^n = \bar{h}, \quad q_i^n = \frac{\bar{h}k}{B_i} \quad \forall i, \tag{24}$$

and

$$B(x_i) = B_i, \quad H_i = H_1 + \frac{k^2}{2g}\left(\frac{1}{B_i^2} - \frac{1}{B_1^2}\right) \quad \forall i. \tag{25}$$

Then the flux and source term discretizations to compute the solution at time $t = t_{n+1}$ are

$$\left(\frac{\phi\left(W_i^n, W_{i+1}^n\right) - \phi\left(W_{i-1}^n, W_i^n\right)}{A_i}\right)_1 = \frac{k\bar{h}}{2A_i}\left(\frac{1}{B_{i+1}} - \frac{1}{B_{i-1}}\right) - \frac{k^2\sqrt{gh}}{4gA_i}\left[\frac{1}{B_{i+1}^2} - \frac{2}{B_i^2} + \frac{1}{B_{i-1}^2}\right] \tag{26}$$

$$\begin{aligned}\left(\frac{\phi\left(W_i^n, W_{i+1}^n\right) - \phi\left(W_{i-1}^n, W_i^n\right)}{A_i}\right)_2 &= \frac{k^2\bar{h}}{2A_i}\left(\frac{1}{B_{i+1}^2} - \frac{1}{B_{i-1}^2}\right) - \frac{k\bar{h}}{2A_i}\sqrt{gh}\left[\frac{1}{B_{i+1}} - \frac{2}{B_i} + \frac{1}{B_{i-1}}\right] \\ &\quad - \frac{k^3\sqrt{gh}}{8gA_i}\left[\left(\frac{1}{B_i} + \frac{1}{B_{i+1}}\right)\left(\frac{1}{B_{i+1}^2} - \frac{1}{B_i^2}\right) - \left(\frac{1}{B_{i-1}} + \frac{1}{B_i}\right)\left(\frac{1}{B_i^2} - \frac{1}{B_{i-1}^2}\right)\right]\end{aligned} \tag{27}$$

$$(G_{i1})_1 = -\frac{k^2\sqrt{gh}}{4gA_i}\left[\frac{1}{B_{i+1}^2} - \frac{2}{B_i^2} + \frac{1}{B_{i-1}^2}\right] \tag{28}$$

$$\begin{aligned}(G_{i1})_2 = \frac{k^2\bar{h}}{4A_i}\left[\frac{1}{B_{i+1}^2} - \frac{1}{B_{i-1}^2}\right] - \frac{k^3\sqrt{gh}}{8gA_i}&\left[\left(\frac{1}{B_i} + \frac{1}{B_{i+1}}\right)\left(\frac{1}{B_{i+1}^2} - \frac{1}{B_i^2}\right)\right. \\ &\left. - \left(\frac{1}{B_{i-1}} + \frac{1}{B_i}\right)\left(\frac{1}{B_i^2} - \frac{1}{B_{i-1}^2}\right)\right]\end{aligned} \tag{29}$$

$$(G_{i2})_1 = \frac{k\bar{h}}{2A_i}\left(\frac{1}{B_{i+1}} - \frac{1}{B_{i-1}}\right) \tag{30}$$

$$(G_{i2})_2 = \frac{k^2\bar{h}}{4A_i}\left[\frac{1}{B_{i+1}^2} - \frac{1}{B_{i-1}^2}\right]. \tag{31}$$

Figures 4 and 5 show the corresponding results obtained with $CFL = 0.9$, $\Delta x = 3\,\mathrm{m}$, and after 500 s, where the steady state is reached. The numerical results for the flow q show diffusive effects (see Fig. 4). Analysis of this effect leads to the conclusion that it is due to the centred discretization used.

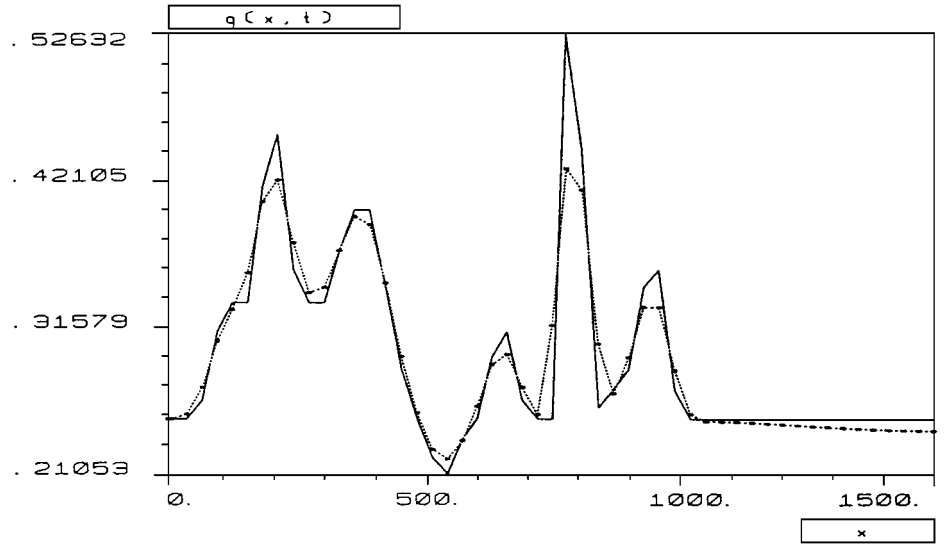

FIG. 4. Flux (q). Q-scheme of van Leer with centred discretization of G_2, $t = 500$ (——— exact solution; -∗- approximate solution).

The stationary problem for which (17)–(18) is a solution, if $M \equiv 0$, is

$$(\mathcal{SP}) \begin{cases} \frac{\partial q}{\partial x} = -q \frac{B'(x)}{B(x)} \\ \frac{\partial}{\partial x}\left(\frac{q^2}{h}\right) = -\frac{q^2}{h}\frac{B'(x)}{B(x)} + g\bar{h}H'(x). \end{cases} \tag{32}$$

A first analysis of the numerical schemes would lead to a test if the two members of (32) were discretized in an analogous way. Next, it will be proved that the difference between

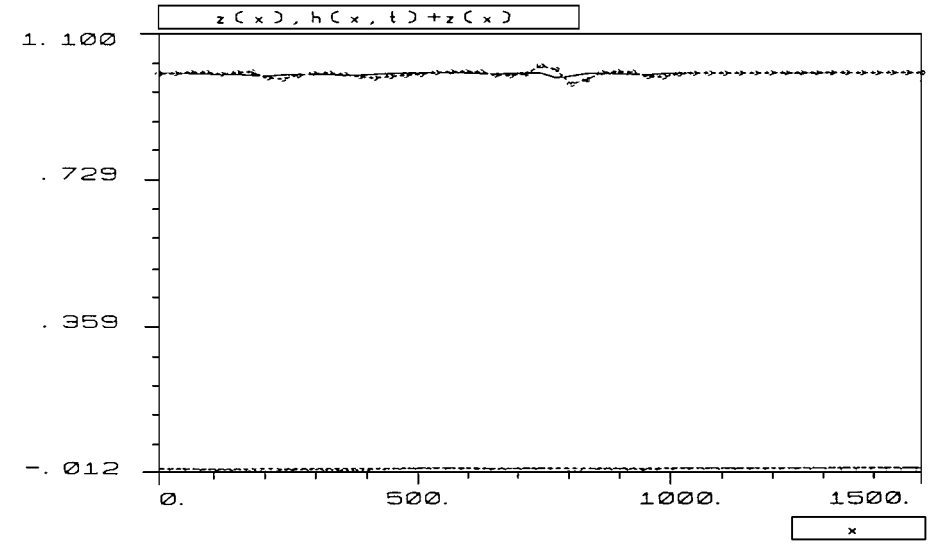

FIG. 5. Profile $(Z(x), h(x,t) + Z(x))$. Q-scheme of van Leer with centred discretization of G_2, $t = 500$ (——— exact solution; -○- approximate solution).

both discretizations are terms of order one in space. Taking the expressions (24)–(29) into account this difference can be written

$$\frac{\phi(W_i^n, W_{i+1}^n) - \phi(W_{i-1}^n, W_i^n)}{A_i} - \sum_{k=1}^{2} G_{ik} = \begin{pmatrix} 0 \\ -\frac{k\bar{h}}{2A_i}\sqrt{gh}\left[\frac{1}{B_{i+1}} - \frac{2}{B_i} + \frac{1}{B_{i-1}}\right] + O(\Delta x)^2 \end{pmatrix}. \tag{33}$$

Thus, to first order, the difference between (32) and (33) is the diffusive term arising from the upwinded flux discretization,

$$-\Delta x \left(\sqrt{gh}\, q_x\right)_x$$

which, in this case, is equal to

$$-\Delta x \left(\sqrt{gh}\, q \frac{B'(x)}{B(x)}\right)_x.$$

In other words, the equivalent, or "modified," equation corresponding to the second equation of the stationary problem (32) and arising from upwinding the flux and G_1 discretization and from a centred discretization of G_2 is

$$\frac{\partial}{\partial x}\left(\frac{q^2}{h}\right) = -\frac{q^2}{h}\frac{B'(x)}{B(x)} + g\bar{h}H'(x) - \Delta x \frac{\partial}{\partial x}\left(\sqrt{gh}\frac{\partial q}{\partial x}\right). \tag{34}$$

It can also be shown that the diffusive effect in q vanishes when a centred discretization of $\Delta x(\sqrt{gh}\, q_x)_x$ is introduced, which cancels the analogous term in (33). In that case, the error term in h is also cancelled. If this cancellation does not occur, the error introduced in h can be seen in Fig. 5.

In relation to the discretization of G_3, taking into account the expression for the depth (19), we observe a term whose derivative is analogous to G_3. Hence, since we have concluded in previous papers the importance of upwinding G_1, it seems reasonable to upwind this source term also. In any case, if we compute the difference between a centred discretization of G_3 and the upwind discretization of the analogous term in G_1 we obtain, for a uniform mesh,

$$\Delta x \frac{g^2 M^2 R_h^{-4/3} k|k|}{4\sqrt{gh}} 6 q_{xxx}, \tag{35}$$

which is a dispersive term.

The expression considered in this paper for the hydraulic radius is that proposed by the *working group on dam break modelling* [9],

$$R_h = \frac{A}{P} = \frac{B(x)h(x,t)}{B(x)} = h; \tag{36}$$

that is, the perimeter P is only the breadth. Nevertheless the conclusions of this study are

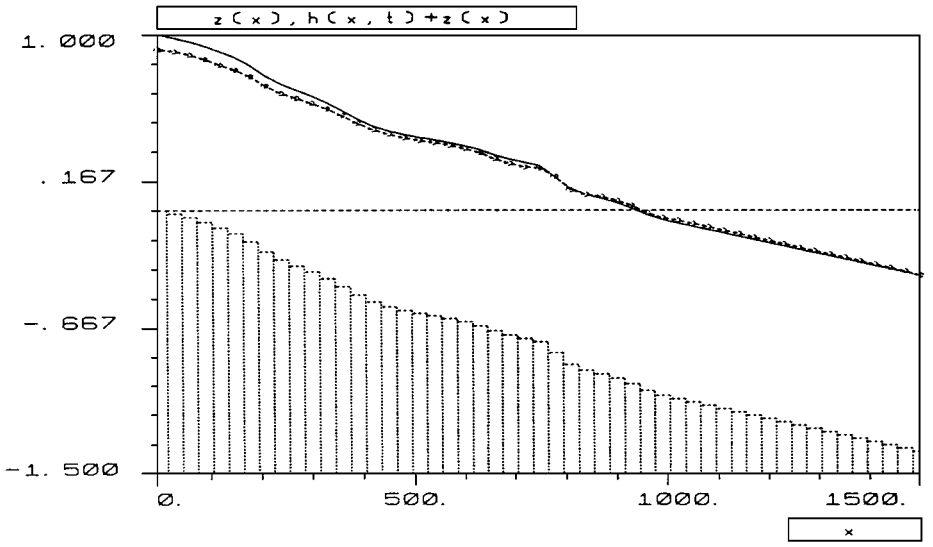

FIG. 6. Profile $(Z(x), h(x,t)+Z(x))$. Q-scheme of van Leer with centred discretization of G_2 and G_3, $M=0.1$ (——— exact solution; -○- approximate solution).

also valid for the expression

$$R_h = \frac{B(x)h(x,t)}{B(x)+2h(x,t)}. \tag{37}$$

Using the previous test case but now with friction, with the Manning coefficient M = 0.1, we see in Fig. 7, not only the regularizing effect due to the centred discretization of G_2, but also a new effect due to the dispersive term related to the centred discretization of G_3 (see also Fig. 6). Also in this case $CLF = 0.9$ and $\Delta x = 3$ m.

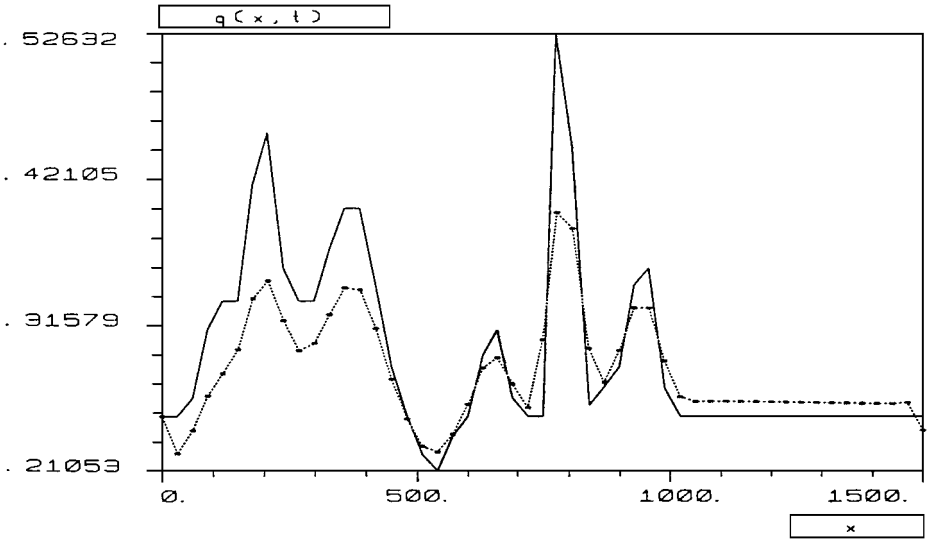

FIG. 7. Flux (q). Q-scheme of van Leer with centred discretization of G_2 and G_3, $M = 0.1$ (——— exact solution; -∗- approximate solution).

In order to avoid these bad effects, upwind discretizations for all source terms will be used. In the next section we will prove that the new scheme computes the stationary solution exactly, or with order greater than one.

3.3. *Upwind Discretizations of the Source Terms*

We now describe in detail the definitions proposed in Vázquez-Cendón [22] to upwind the source terms for general meshes:

- The integral of G_k over the cell C_i is split in the sum of two integrals on the subcells $T_{i\mathrm{L}}$ and $T_{i\mathrm{R}}$,

$$\frac{1}{A_i}\int_{C_i} G_k(x, W^n)\,dx = \frac{1}{A_i}\left[\int_{T_{i\mathrm{L}}} G_k(x, W^n)\,dx + \int_{T_{i\mathrm{R}}} G_k(x, W^n)\,dx\right], \quad k = 1, 2, 3, \tag{38}$$

where $T_{i\mathrm{L}} = (x_{i-1/2}, x_i)$ and $T_{i\mathrm{R}} = (x_i, x_{i+1/2})$ are subcells of the cell C_i, as has been detailed in Fig. 2.

- Continuous functions $\hat{G}_k$, $k = 1, 2, 3$, giving an average of G_k on the subcells $T_{i\mathrm{L}}$ and $T_{i\mathrm{R}}$ are defined. Then $\hat{G}_k$, $k = 1, 2, 3$, also depend on the contiguous nodes. The discretization of the source terms is then given by

$$\frac{1}{A_i}\left[A_{T_{i\mathrm{L}}}\hat{G}_k\left(x_{i-1}, x_i, W^n_{i-1}, W^n_i\right) + A_{T_{i\mathrm{R}}}\hat{G}_k\left(x_i, x_{i+1}, W^n_i, W^n_{i+1}\right)\right], \quad k = 1, 2, 3, \tag{39}$$

where $A_{T_{i\mathrm{L}}} = (x_i - x_{i-1})/2$ and $A_{T_{i\mathrm{R}}} = (x_{i+1} - x_i)/2$ denote the length of $T_{i\mathrm{L}}$ and $T_{i\mathrm{R}}$, respectively.

- Finally, to obtain an upwind discretization of the source terms it only remains to define $\psi_{\mathrm{L}k}$ and $\psi_{\mathrm{R}k}$, $k = 1, 2, 3$. These functions will give upwind values of the source terms on both sides of node x_i, on the subcells $T_{i\mathrm{L}}$ and $T_{i\mathrm{R}}$, respectively. In summary, we propose an upwind definition of the source terms as

$$G^n_{ki} = \frac{1}{A_i}\left[A_{T_{i\mathrm{L}}}\psi_{\mathrm{L}k}\left(x_{i-1}, x_i, W^n_{i-1}, W^n_i\right) + A_{T_{i\mathrm{R}}}\psi_{\mathrm{R}k}\left(x_i, x_{i+1}, W^n_i, W^n_{i+1}\right)\right], \quad k = 1, 2, 3. \tag{40}$$

In Bermúdez and Vázquez [3] the following source functions are proposed:

$$\psi_{\mathrm{L}k}(x, y, V, W) = [I + |Q(V, W)|Q^{-1}(V, W)]\hat{G}_k(x, y, V, W) \tag{41}$$

$$\psi_{\mathrm{R}k}(x, y, V, W) = [I - |Q(V, W)|Q^{-1}(V, W)]\hat{G}_k(x, y, V, W). \tag{42}$$

For the functions $\hat{G}_k$ the following is proposed:

$$\hat{G}_k(x, y, V, W) = G_k\left(\frac{x + y}{2}, \frac{V + W}{2}\right), \quad k = 1, 2, 3. \tag{43}$$

We have described the construction of the schemes and, knowing the form of the source terms, it is only necessary to make precise the approximation to the derivative or to the integral of the functions which appear in the centred source terms $\hat{G}_k$, $k = 1, 2, 3$. Even if we know analytical expressions for these functions,for the sake of consistency we shall use

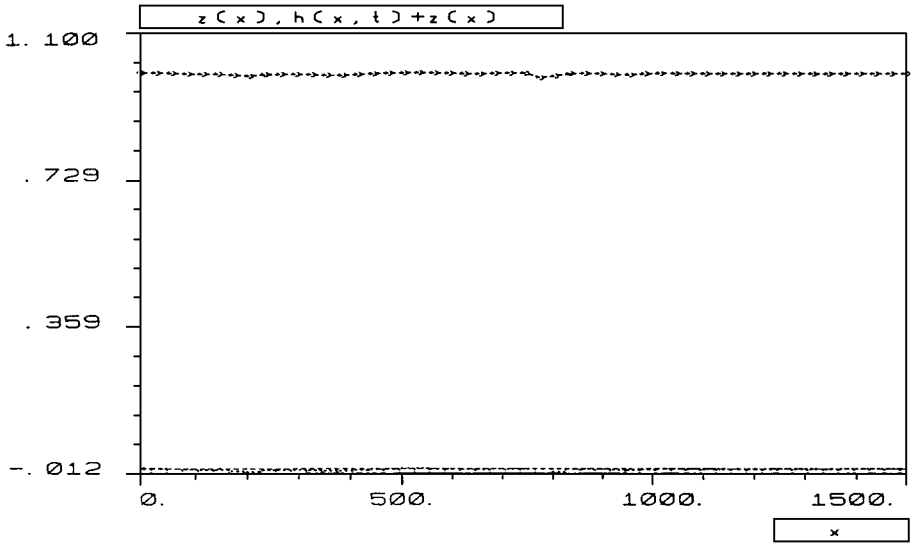

FIG. 8. Profile $(Z(x), h(x,t)+Z(x))$. Extension of the Q-scheme of van Leer $t=500$, $M=0$ (——— exact solution; -○- approximate solution).

the approximations:

$$H'\left(\frac{x+y}{2}\right) \approx \frac{H(y)-H(x)}{y-x} \tag{44}$$

$$B'\left(\frac{x+y}{2}\right) \approx \frac{B(y)-B(x)}{y-x} \tag{45}$$

$$\int_x^y \frac{1}{B^2(s)}\,ds \approx \left(\frac{1}{B^2(x)}+\frac{1}{B^2(y)}\right)\frac{(y-x)}{2}. \tag{46}$$

We now present the results obtained with these approximations for the test problem presented at the beginning of this section: The CFL number is 0.9 and $\Delta x = 3$ m without friction ($M=0$) in Figs. 8 and 9; and with friction ($M=0.1$) in Figs. 10 and 11. In either of the two cases[1] a considerable increase in accuracy can be observed, particularly for the case without friction ($M=0$), where no difference between the exact and the approximate solution can be seen, and even if $M=0.1$, we can also observe the efficiency of the proposed extensions.

Later on in this paper, in the section devoted to the conservation property, we will refer back to the stationary solution (17)–(18) and give a more rigorous interpretation of the numerical results.

Next we study the consistency of the proposed extensions. In order to do this we recall the definition of consistency relative to the discretizaton of the source terms introduced in Vázquez-Cendón [22] for nonuniform meshes.

[1] As has already been mentioned, for these solutions the Q matrix is the same for the two schemes considered, and so only the results corresponding to the Q-scheme of van Leer are shown.

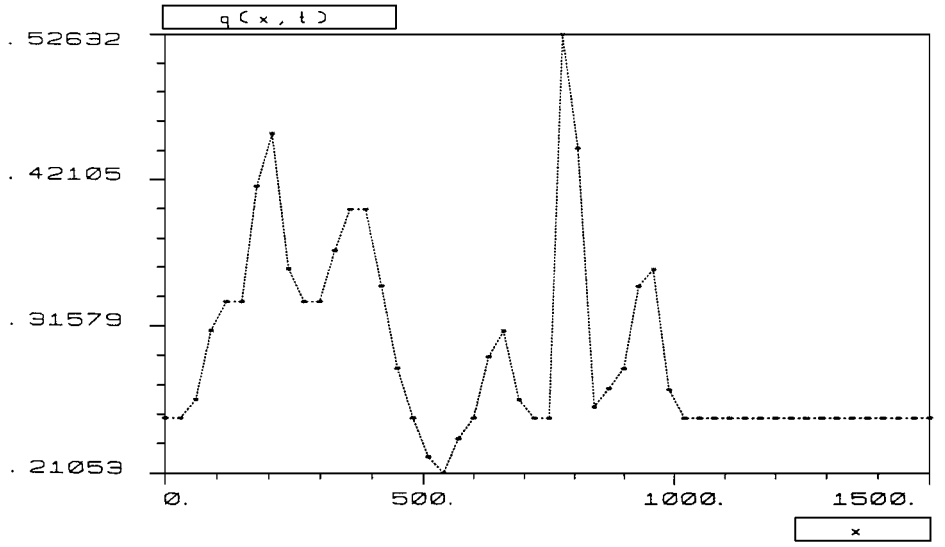

FIG. 9. Flux (q). Extension of the Q-scheme of van Leer $t = 500$, $M = 0$ (——— exact solution; -∗- approximate solution).

Consistency. As is well known, the numerical flux ϕ of an upwind scheme is *consistent with the continuous flux F* (see, for instance, [8]) if the following equality holds:

$$\phi(W, W) = F(W) \quad \forall W \in \mathbb{R}^p. \tag{47}$$

In the case of $G \equiv 0$, this definition coincides with the classical notion of consistency; that is, the discretization error goes to zero when Δx goes to zero.

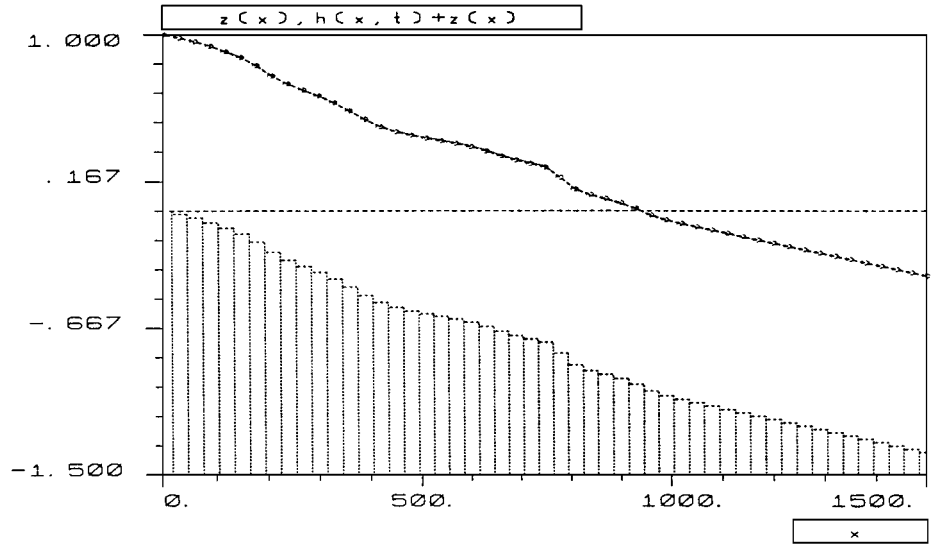

FIG. 10. Profile $(Z(x), h(x,t) + Z(x))$. Extension of the Q-scheme of van Leer $t = 500$, $M = 0.1$ (——— exact solution; -○- approximate solution).

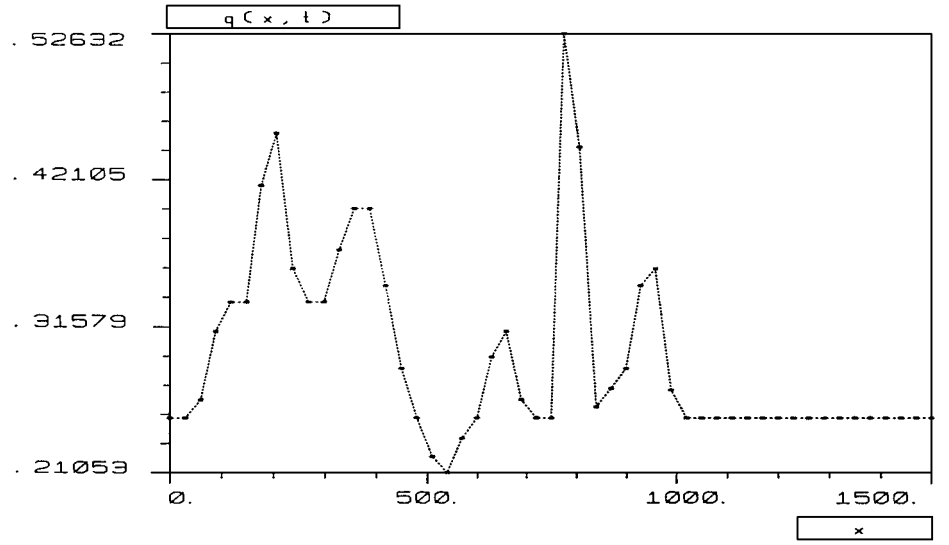

FIG. 11. Flux (q). Extension of the Q-scheme of van Leer $t = 500$, $M = 0.1$ (——— exact solution; -∗- approximate solution).

If $G \not\equiv 0$ we introduce the following definition:

DEFINITION 1. The discretization of the source terms given by (40) is said to be consistent if it satisfies

$$\lim_{\substack{\Delta x \to 0 \\ U,V \to W}} \frac{1}{A_i} \left[A_{T_{i\mathrm{L}}} \psi_{\mathrm{L}k}(x_{i-1}, x_i, U, W) + A_{T_{i\mathrm{R}}} \psi_{\mathrm{R}k}(x_i, x_{i+i}, W, V) \right] - G_k(x_i, W) = 0$$

$$\forall i;\ k = 1, 2, 3. \quad (48)$$

In what follows, necessary conditions to obtain consistency in the sense of Definition 1 are detailed.

Let us remark that the mesh can be nonuniform. In this case, to obtain consistency it is necessary that the mesh satisfy the property of *asymptotic local uniformity*:

$$\lim_{\Delta x \to 0} \frac{|x_i - x_{i+1}|}{|x_i - x_{i-1}|} = 1 \quad \forall i. \quad (49)$$

Then it is easy to prove that, if $\{\mathcal{C}_{\Delta x}\}$ is a family of meshes with property (49) and ψ_{L} and ψ_{R} are continuous functions, the discretization of the source terms given by (40) is consistent with the source terms if and only if the numerical source functions satisfy the relation

$$\frac{\psi_{\mathrm{L}k}(x, x, W, W) + \psi_{\mathrm{R}k}(x, x, W, W)}{2} = G_k(x, W), \quad k = 1, 2, 3. \quad (50)$$

It is obvious that the source terms defined previously satisfy the relations given in (50) so that we have consistency of the schemes.

4. A $\mathcal{C}$-PROPERTY RELATIVE TO A STATIONARY SOLUTION

In previous papers [3, 2] devoted to the numerical solution of the shallow water equations only the source term involving the bed slope is taken into account. A centred discretization

of this term gives rise to spurious waves. The analysis of this phenomenon brings about the definition of a "conservation property" introduced by Bermúdez and Vázquez in [3]. This definition characterizes the order with which a numerical scheme approximates a steady solution representing water at rest ($h \equiv H$, $q \equiv 0$). In this solution the importance of the term G_1 is noted. If the conservation property is not satisfied (exactly or approximately), then the propagation of spurious waves in nonstationary problems is also detected. Moreover, the idea of this property is to preserve what Greenberg and LeRoux defined in [10] as a "well-balanced scheme." It is also related to the "piecewise stationary" discretization of the source term proposed first by Liu [15] and then by van Leer in [21].

If we try to apply the same definition of the conservation property to the present problem, for which G_2 and G_3 are nonzero, this property does not allow us to analyze of the new source terms.

Nevertheless, a *new* conservation property relative to a stationary solution can be introduced which helps to analyze all the three source terms G_1, G_2, and G_3. The stationary solution is the one introduced in the previous section.

After concluding in the previous section that a first-order approximation of this solution should not be enough for conservation (unless Δx was notably reduced) to obtain good results, the following definitions are introduced.

DEFINITION 2. We say that a scheme satisfies the exact $\mathcal{C}$-property regarding the stationary solution (17)–(18) if it is exact when applied to the stationary problem ($\mathcal{SP}$) given in Section 3.

DEFINITION 3. We say that a scheme satisfies the approximate $\mathcal{C}$-property regarding the stationary solution (17)–(18) if it is accurate to order $O(\Delta x^2)$ when applied to the stationary problem ($\mathcal{SP}$) given in Section 3.

The behaviour of the different schemes from the point of view of these two $\mathcal{C}$-properties is as follows:

(i) The Q-schemes of Roe and van Leer with centred approximations of any of the source terms (G_k, $k = 1, 2, 3$) applied to the shallow water equations do not satisfy either the exact nor the approximate $\mathcal{C}$-property relating to the stationary solution (17)–(18). This is a consequence of the first-order terms described in a previous section and in [3].

(ii) The extensions of the Q-schemes of Roe and van Leer applied to the shallow water equations satisfy the approximate $\mathcal{C}$-property relating the stationary solution (17)–(18) if we use the expression of H given by (19) and the approximations (44)–(46). Proceeding as in the previous section for the different cases of (subcritical and supercritical) flow, the proof of this statement is obtained. More specifically, the difference between the discretization of flux and source terms is $O(\Delta x)^2$ in the two components, with the Manning coefficient as a factor multiplying this difference. Hence, the following statement is obtained.

(iii) If the friction effect is neglected and the approximations (44) and (45) are considered, then these schemes satisfy the exact $\mathcal{C}$-property relating to the stationary solution (17)–(18) if we consider the expression of H given by (19).

This behaviour has been shown numerically throughout the previous section. Figures 4–7 are related to (i) for which $\mathcal{C}$-property does not hold. The exact $\mathcal{C}$-property is satisfied without friction as in (iii), which is the case in Figs. 8–9. Finally the approximate $\mathcal{C}$-property is obtained when upwind discretizations for all of the source terms are considered, as has been seen in Figs. 10–11.

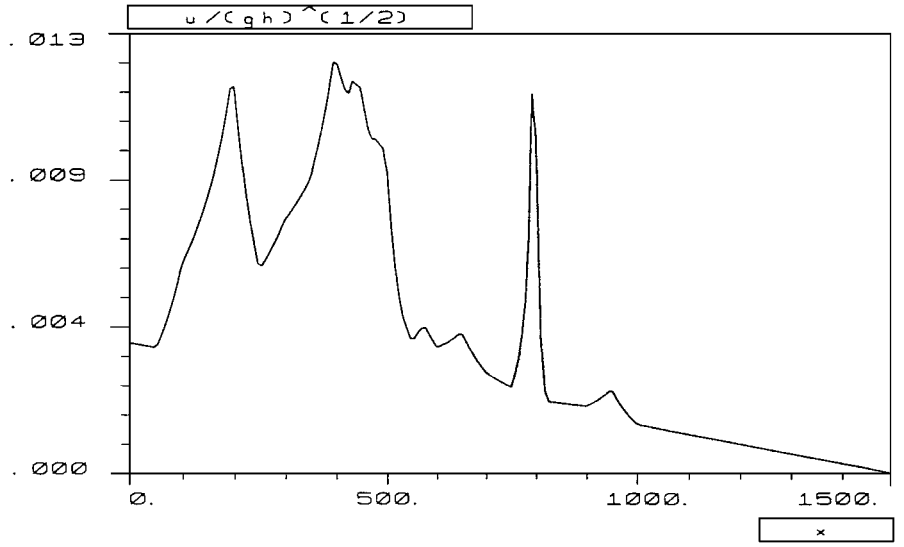

FIG. 12. Froude number. Extension of the Roe scheme $t = 10{,}800$, $M = 0.1$, 200 nodes.

5. NUMERICAL RESULTS

5.1. *An Asymptotic Analytical Solution for Small Froude Numbers*

In previous sections we have analyzed the behaviour of the new schemes in the case of stationary solutions. In order to show that the conservation property is also a good test for unsteady problems a transient solution for a small Froude number is obtained in this section (see Fig. 12).

This solution offers the possibility of comparing the schemes in a test including variable depth and breadth functions. In the bibliography we have not found any exact analytical solution for the shallow water equations when the geometry changes in that way.

More precisely, in this paper a generalization of the "asymptotic" solution given in Bermúdez and Vázquez [3] for the case $B \equiv 1$ is proposed. For small Froude numbers an asymptotic solution can be obtained. For this purpose it is convenient to write the equations in a nondimensional form. This can be done by using typical values of time, space, depth, breadth, and velocity, $T^\star$, $L^\star$, $H^\star$, $B^\star$, $U^\star$, respectively, to define new variables and functions

$$\hat{t} = \frac{t}{T^\star}, \quad \hat{x} = \frac{x}{L^\star}, \quad \hat{h} = \frac{h}{H^\star}, \quad \hat{H} = \frac{H}{H^\star}, \quad \hat{B} = \frac{B}{B^\star}, \quad \hat{u} = \frac{u}{U^\star}, \quad \hat{q} = \hat{h}\hat{u}.$$

Thus (5) becomes

$$\frac{\partial \hat{h}}{\partial \hat{t}} + \frac{T^\star U^\star}{L^\star}\frac{\partial \hat{q}}{\partial \hat{x}} = -\hat{q}\frac{T^\star U^\star}{L^\star}\frac{\hat{B}'(\hat{x})}{\hat{B}(\hat{x})} \tag{51}$$

$$\frac{\partial \hat{q}}{\partial \hat{t}} + \frac{T^\star U^\star}{L^\star}\frac{\partial}{\partial \hat{x}}\left(\frac{\hat{q}^2}{\hat{h}} + \frac{1}{2\mathcal{F}^2}\hat{h}^2\right) = \frac{T^\star U^\star}{L^\star}\frac{1}{\mathcal{F}^2}\hat{h}\hat{H}'(\hat{x}) - \frac{T^\star U^\star}{L^\star}\frac{\hat{q}^2}{\hat{h}}\frac{\hat{B}'(\hat{x})}{\hat{B}(\hat{x})} - T^\star U^\star H^{\star -\frac{4}{3}}\hat{h}^{-\frac{4}{3}}\hat{q}|\hat{u}|M^2 g, \tag{52}$$

where $\mathcal{F}$ denotes the Froude number. As is well known, this number represents the ratio

between the velocity of particles and the velocity of gravity waves and is given by

$$\mathcal{F} = \frac{U^\star}{\sqrt{gH^\star}}. \tag{53}$$

Suppose we are concerned with a "relatively short" domain $L^\star$ for which $T^\star \sim L^\star/U^\star$, so that (51)–(52) becomes

$$\frac{\partial \hat{h}}{\partial \hat{t}} + \frac{\partial \hat{q}}{\partial \hat{x}} = -\hat{q}\frac{\hat{B}'(\hat{x})}{\hat{B}(\hat{x})} \tag{54}$$

$$\frac{\partial \hat{q}}{\partial \hat{t}} + \frac{\partial}{\partial \hat{x}}\left(\frac{\hat{q}^2}{\hat{h}} + \frac{1}{\mathcal{F}^2}\frac{\hat{h}^2}{2}\right) = \frac{1}{\mathcal{F}^2}\hat{h}\hat{H}'(\hat{x}) - \frac{\hat{q}^2}{\hat{h}}\frac{\hat{B}'(\hat{x})}{\hat{B}(\hat{x})} - L^\star H^{\star -4/3}\hat{h}^{-4/3}\hat{q}|\hat{u}|M^2 g. \tag{55}$$

Now we assume $\mathcal{F}$ is small, which is the case for strongly subcritical flows, and we try to obtain an approximate solution of (55) by asymptotic analysis. By replacing $\hat{h}$ and $\hat{q}$ in (54)–(55) by asymptotic expansions with respect to the small parameter $\mathcal{F}$ and then identifying the terms of the same degree we easily obtain, for the lowest order terms $\hat{h}_0$ and $\hat{q}_0$, the equations

$$\frac{\partial \hat{h}_0}{\partial \hat{t}} + \frac{\partial \hat{q}_0}{\partial \hat{x}} = -\hat{q}\frac{\hat{B}'(\hat{x})}{\hat{B}(\hat{x})} \tag{56}$$

$$\hat{h}_0\frac{\partial \hat{h}_0}{\partial \hat{x}} = \hat{h}_0\hat{H}'(\hat{x}), \tag{57}$$

together with the boundary conditions

$$\hat{h}_0(0,\hat{t}) = \hat{\varphi}(\hat{t}) + \hat{H}(0) \tag{58}$$

$$\hat{q}_0(L,\hat{t}) = \hat{\psi}(\hat{t}). \tag{59}$$

By integrating (56)–(57) and then returning to the primitive variables, we obtain the first-order approximate solution to (51)–(52):

$$h_0(x,t) = \varphi(t) + H(x) \tag{60}$$

$$q_0(x,t) = \psi(t) + \frac{\varphi'(t)}{B(x)}\int_x^L B(s)\,ds \tag{61}$$

which can be compared to the numerical solution obtained by using the schemes considered in Section 3 for small $\mathcal{F}$. Let us remark that to obtain (61) it is necessary to take into account that (56) is equivalent to

$$\hat{B}(x) + \frac{\partial \hat{h}_0}{\partial t} + \frac{\partial \hat{Q}_0}{\partial \hat{x}} = 0, \tag{62}$$

where $\hat{Q}_0 = \hat{B}\hat{q}_0$.

TABLE II
Values of Bed Function at the Points *x*

x	0	50	100	150	200	250	300	350	400	425	435	450	470	475	500
$Z(x)$	0	0	2.5	5	5	3	5	5	7.5	8	9	9	9	9.1	9
x	505	530	550	565	575	600	650	700	750	800	820	900	950	1000	1500
$Z(x)$	9	6	5.5	5.5	5	4	3	3	2.3	2	1.2	0.4	0	0	0

5.2. *Propagation of a Tidal Wave in a "Relatively Short" Channel with Variable Depth and Breadth*

As a numerical test we compute the propagation of a tidal wave in a "relatively short" channel ($L^\star \sim U^\star T^\star$) with variable depth. More precisely, we take as the geometric domain of the flow an interval of $L = 1500$ m. The initial and boundary conditions are taken to be

$$h(x, 0) = H(x) \tag{63}$$

$$q(x, 0) = 0 \tag{64}$$

and

$$h(0, t) = H(0) + 4 + 4 \sin\left(\pi\left(\frac{4t}{86,400} - \frac{1}{2}\right)\right) \tag{65}$$

$$q(L, t) = 0, \tag{66}$$

respectively. Equation (65) simulates a tidal wave of 4 m amplitude.

To illustrate the behaviour of the proposed schemes with nonsmooth depth and breadth functions the piecewise linear functions are defined. The breadth function is that considered in Section 2 (see Fig. 3 and Table I). For the depth the following elections are proposed: the first one (see Table II) is the same bed of the channel that has been proposed by the *working group on dam break modelling* [9], and the second one (see Eq. (67)) tries to take into account critical slope values:

$$Z(x) = \begin{cases} 8, & \text{if } \left|x - \frac{1500}{2}\right| \le \frac{1500}{8}, \\ 0, & \text{otherwise.} \end{cases} \tag{67}$$

The results from the extensions of the two Q-schemes are shown in Figs. 13–16 with CFL $= 0.9$ and 200 nodes. To illustrate that the conservation property is a good way to monitor the behaviour of the schemes for unsteady flows, centred discretization of all the source terms are also presented (see Figs. 17, 18) to compare them with the upwind ones.

As can be detected in the figures associated with the profile, the bed given by Table II is consider in the results obtained with the Roe scheme (Figs. 12–14, 17–18) and the other one given by (67) is used with the Q-scheme of van Leer (Figs. 15–16).[2]

The two instants chosen are $t = 10{,}800$ s which corresponds with the half-risen tide and the maximum positive velocities, and $t = 32{,}400$ s which corresponds with the half-ebb tide and the maximum negative velocities.

[2] This selection is not related with the properties of the schemes; it is only to restrict the number of figures. In both cases the performances of the schemes are similar.

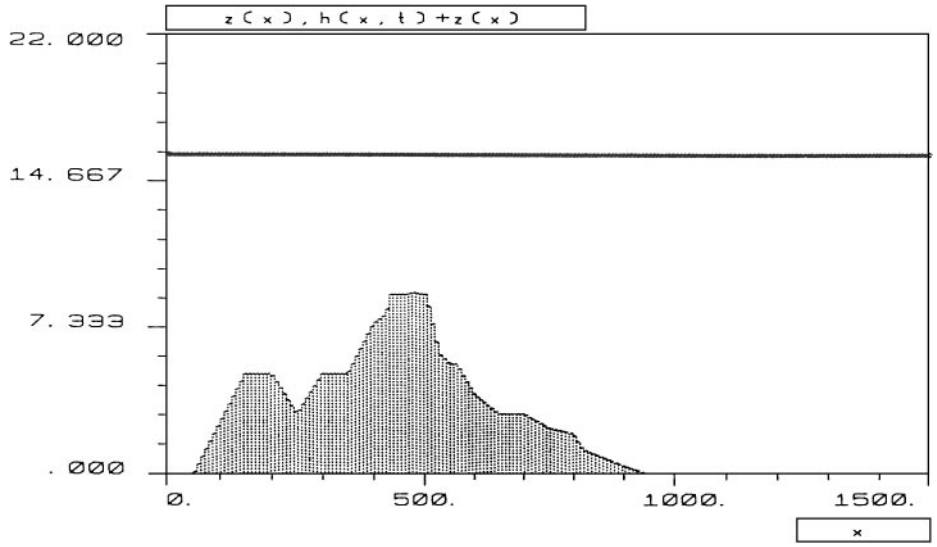

FIG. 13. Profile $(Z(x), h(x,t)+Z(x))$. Extension of the Roe scheme $t = 10{,}800$, $M = 0.1$ (——— exact solution; -○- approximate solution).

Figure 12 shows that the values of the Froude number are small, as has been assumed in the previous section.

Observe that the extensions of the Q-schemes give good results when compared to the asymptotic analytical solution (60)–(61). On the other hand, centred discretizations of the source terms G_k, $k = 1, 2, 3$, lead to numerical results with too high spatial differences in water level and flux. One reason for this bad behaviour is that the latter schemes do not satisfy either the exact or the approximate $\mathcal{C}$-property.

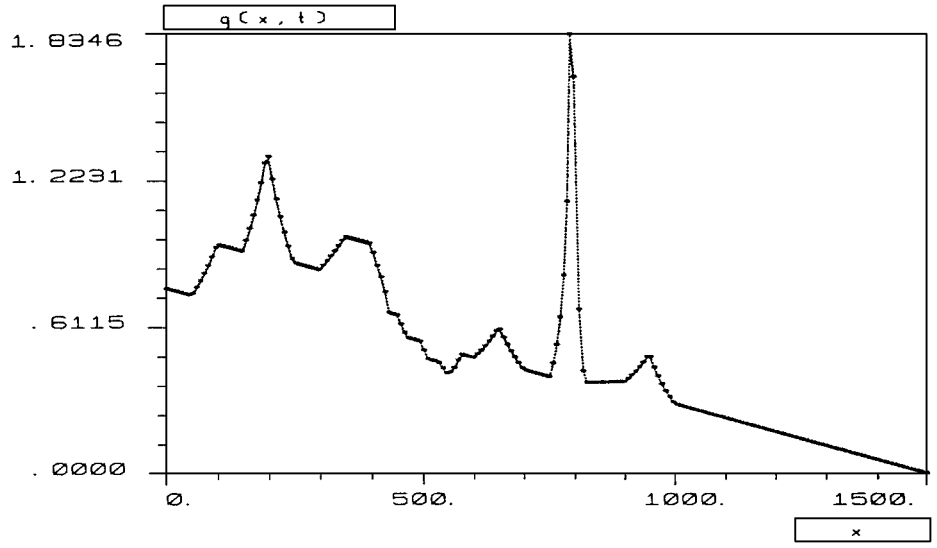

FIG. 14. Flux (q). Extension of the Roe scheme $t = 10{,}800$, $M = 0.1$ (——— exact solution; -∗- approximate solution).

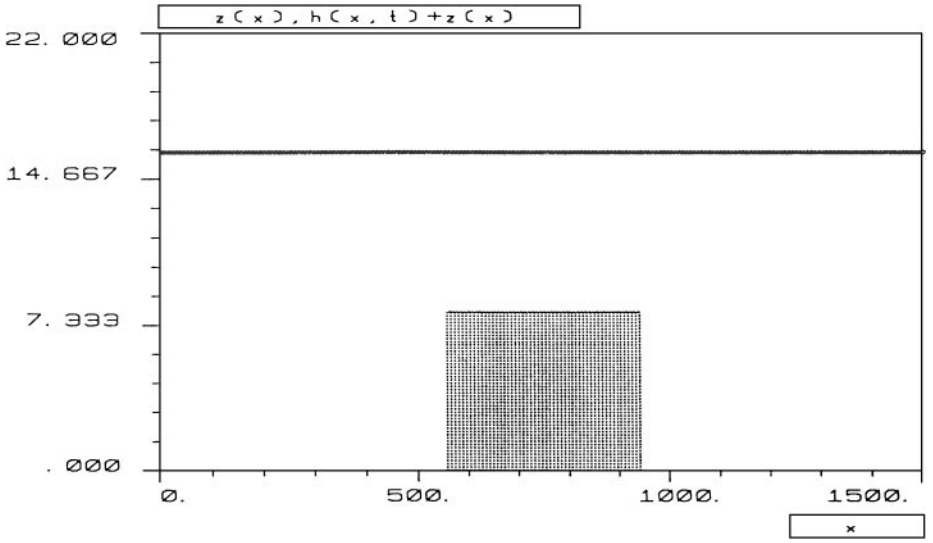

FIG. 15. Profile $(Z(x), h(x,t)+Z(x))$. Extension of the Q-scheme of van Leer $t=32{,}400$, $M=0.1$ (——— exact solution, -○- approximate solution).

The main aim of these two last subsections is to test the numerical schemes with relevant problems presented in the literature.

5.3. *The Steady Flow over a Bump in a Rectangular Channel*

The purpose of this problem is to calculate the steady flow over a bump in a rectangular channel with constant breadth. It is a classical test problem and it has been considered, for example, by the *working group on dam break modelling* [9], where it is also detailed how to compute the analytical solutions.

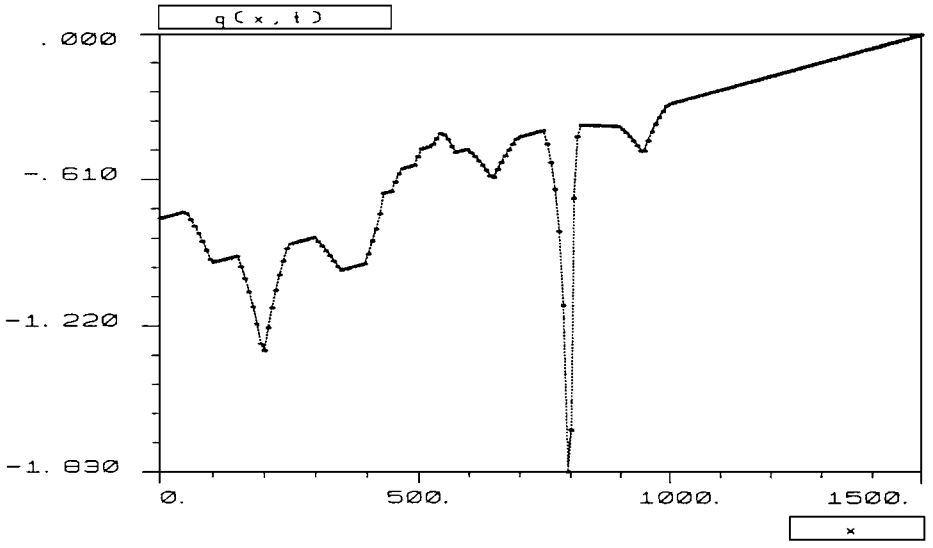

FIG. 16. Flux (q). Extension of the Q-scheme of van Leer $t=32{,}400$, $M=0.1$ (——— exact solution; -∗- approximate solution).

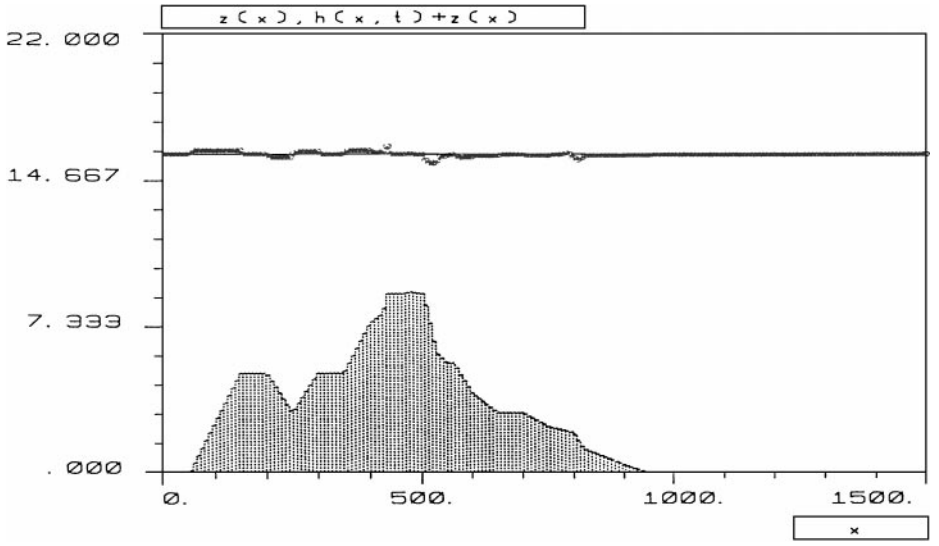

FIG. 17. Profile $(Z(x), h(x,t)+Z(x))$. Roe scheme and centred discretization of the source terms $t = 10{,}800$, $M = 0.1$ (——— exact solution; -○- approximate solution).

The breadth of the channel is constant, $B(x) = 1$ m, the length is $L = 25$ m and the bottom topography is given by

$$Z(x) = \begin{cases} 0.2 - 0.05(x-10)^2, & \text{if } 8 < x < 12, \\ 0, & \text{otherwise.} \end{cases} \tag{68}$$

According to the boundary and initial conditions, the flow may be subcritical, transcritical with a steady shock, or supercritical.

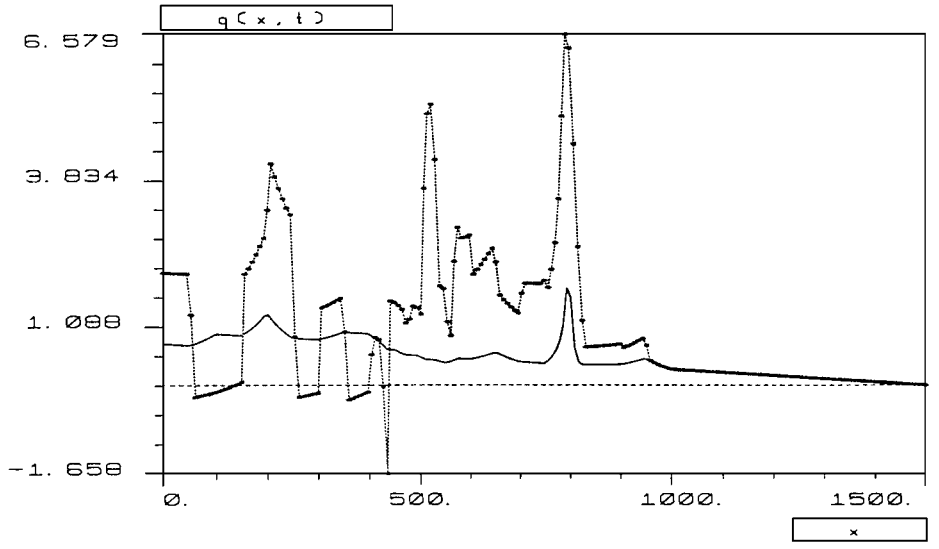

FIG. 18. Flux (q). Roe scheme and centred discretization fof the source terms $t = 10{,}800$, $M = 0.1$ (——— exact solution; -∗- approximate solution).

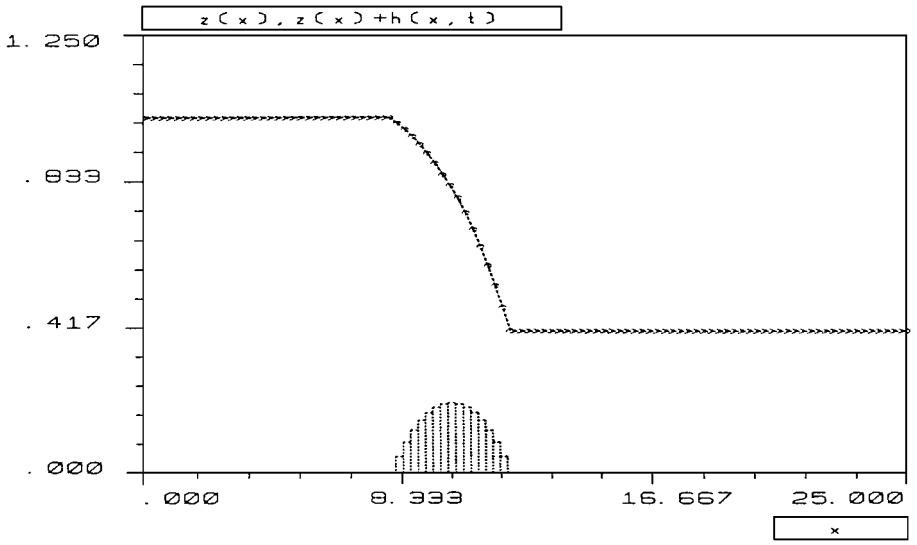

FIG. 19. $Z(x), h(x,t)+Z(x)$ Transcritical flow without shock. Extension of the Q-scheme of van Leer (——— exact solution; -○- approximate solution).

- Transcritical flow without shock (Fig. 19):

  —Downstream. The water level $h = 0,66$ m is imposed only when the flow is subcritical.

  —Upstream. The discharge is imposed $Q = 1.53$ m^3/s.
- Transcritical flow with shock (Fig. 20):

  —Downstream. The water level $h = 0,33$ m is imposed.

  —Upstream. The discharge $Q = 0.18$ m^3/s is imposed.

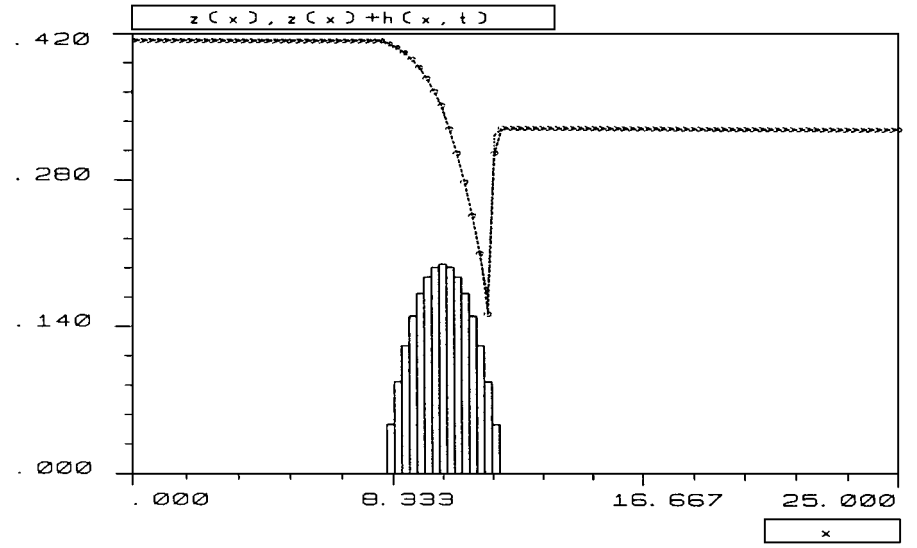

FIG. 20. $Z(x), h(x,t)+Z(x)$ Transcritical flow with shock. Extension of the Q-scheme of van Leer (——— exact solution; -○- approximate solution).

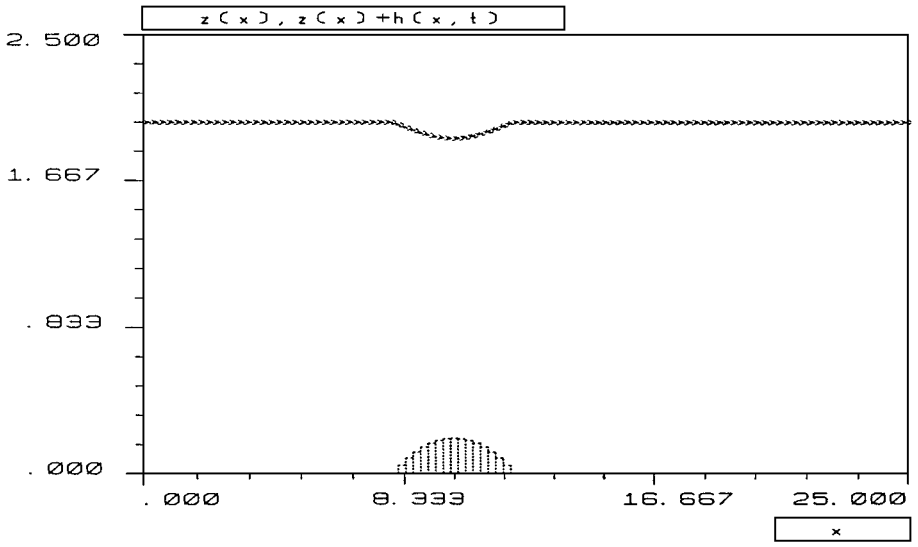

FIG. 21. $Z(x)$, $h(x,t)+Z(x)$ subcritical flow. Extension of the Q-scheme of van Leer (——— exact solution; -○- approximate solution).

- Subcritical flow (Fig. 21):
  —Downstream. The water level $h = 2$ m is imposed.
  —Upstream. The discharge $Q = 4,42$ m^3/s is imposed.

In the three cases as initial conditions we take a constant water level equal to de level imposed downstream and the discharge equal to zero.

To prevent the numerical velocity of the mentioned Q-schemes from vanishing when some of the eigenvalues of the Jacobian matrix of the flux is zero, we apply the Harten regularization (see [11]). The considered the ϵ value given by

$$\epsilon = 0.1\sqrt{gh}. \tag{69}$$

As is well known this regularization is especially important for the transcritical cases near a sonic point. This regularization is only applied to the numerical flux function, not to the numerical source functions.

The comparison of the results with the associated analytical solutions illustrates the improved performance of the discretizations in critical situations. The level of the water is chosen to show the numerical results because it is more relevant than the discharge; it is zero for the three cases. We take CFL $= 1$, $\Delta x = 0.25$ m, $t = 200$ s, where the steady state is reached.

This election of Δx is sufficient to compute the solutions in Figs. 19 and 21 properly. In Fig. 20 the shock can be obtained with more accuracy if the number of nodes is increased. An analogous situation is presented in Fig. 23, where the number of nodes is 200 and the shock is properly computed.

5.4. *A Converging–Diverging Channel*

In order to analyze the behaviour of the schemes in other relevant problems presented in the literature two test cases considereded by P. García-Navarro *et al.* in [4] has been

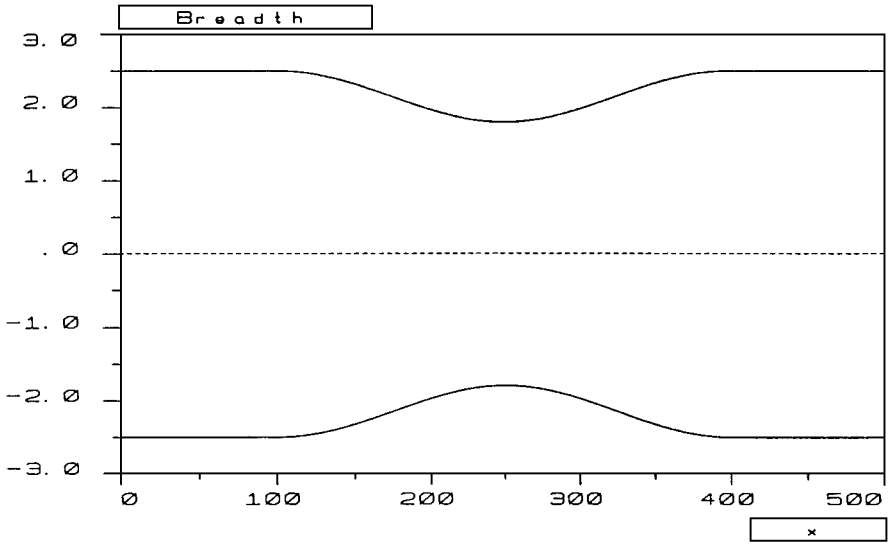

FIG. 22. Breadth of the channel.

selected: a transcritical case in a steady flow and transient motion in supercritical situations in a converging–diverging channel with flat bed.

5.4.1. Steady flow. This is an interesting problem to test the efficiency of the discretization of the source term G_2 involving the breadth of the channel. The width variation modifies the steady-state profiles and due to the boundary conditions a stationary hydraulic jump appears to connect subcritical and supercritical flows. As it is said in [4], these example is related to many practical problems such us flow between bridge piers.

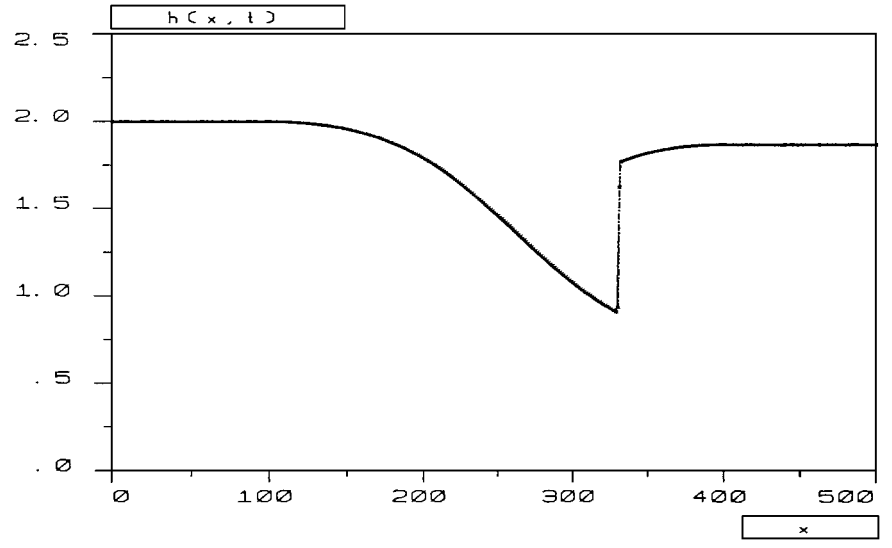

FIG. 23. $h(x, t)$ Extension of the Q-scheme of van Leer (——— exact solution; -∗-·-∗- approximate solution).

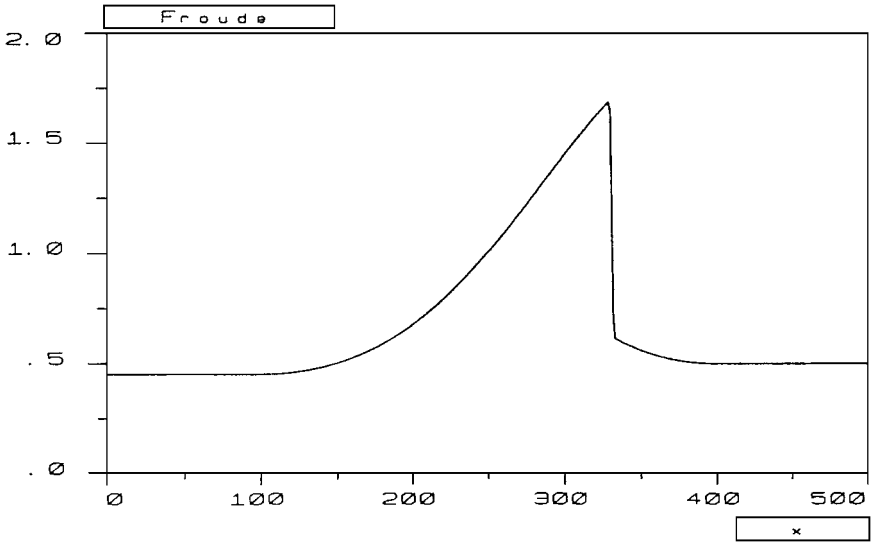

FIG. 24. Froude number.

More precisely, the geometrical domain of the flow is an interval of $L = 500$ m with flat bed ($Z(x) = 0\ \forall x$) and a sinusoidal width variation (see Fig. 22) given by

$$B(x) = \begin{cases} 5 - 0.7065\left(1 + \cos\left(2\pi\left(\frac{x-250}{300}\right)\right)\right), & \text{if } |x - 250| \le 150, \\ 5, & \text{otherwise.} \end{cases} \tag{70}$$

Subcritical initial conditions are stated at a depth $h(x, 0) = 2$ m. As boundary conditions the discharge $Q(0, t) = 20$ cum/s at the upstream and a 0.1 m high weir condition at the downstream boundary are imposed. The numerical results show up the

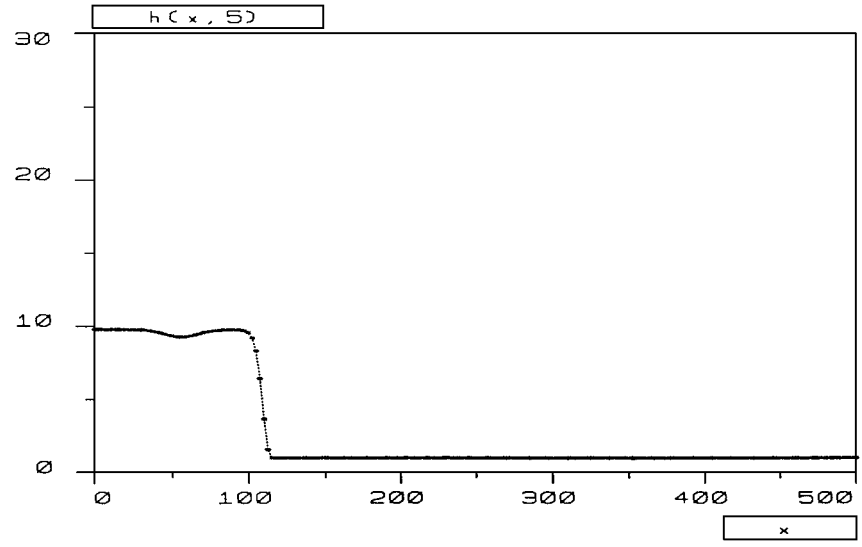

FIG. 25. $h(x, 5)$ Extension of the Q-scheme of van Leer.

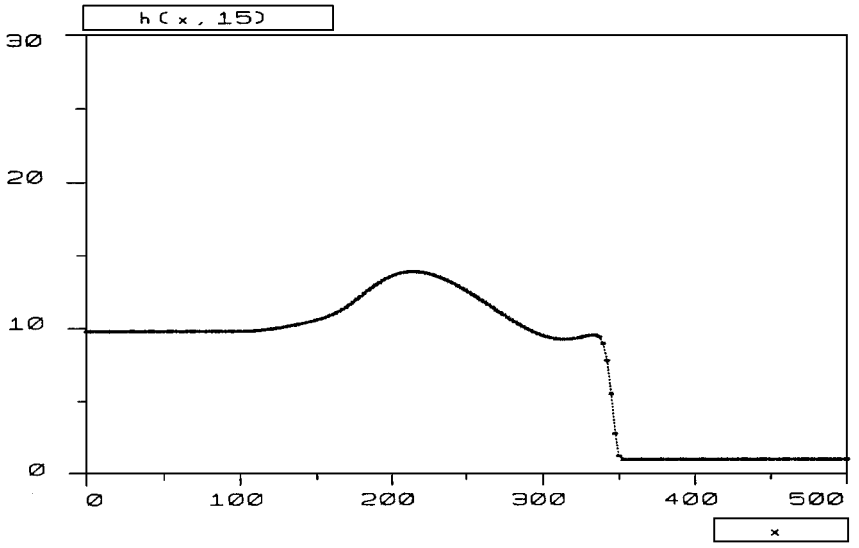

FIG. 26. $h(x, 15)$ extension of the Q-scheme of van Leer.

performances of the new extensions and the exact solution (see [4]) is plotted for comparison. As Fig. 23 shows, the water accelerates as it approaches the point of maximum contraction ($B(250) = 3.587$ m), the flow becomes critical there and it changes then to supercritical flow that gives rise to a stationary hydraulic jump to connect with the subcritical profile required by the downstream condition (see Fig. 24 for the Froude number).

The CFL number considered is 0.9, $\Delta = 2.5$ m, and $M = 0$. The comparison between the exact solution and also the McCormack TVD scheme (second-order accuracy) used by García-Navarro *et al.* in [4] confirms the improved properties of the proposed schemes.

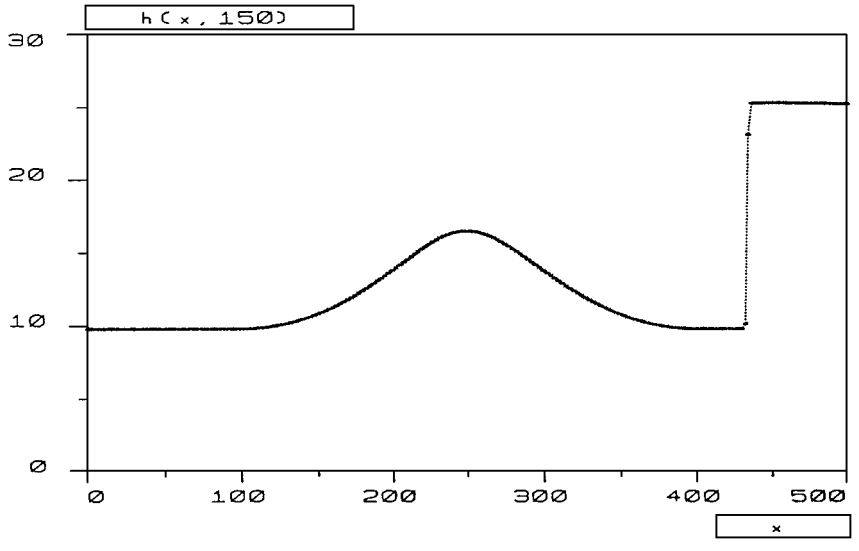

FIG. 27. $h(x, 150)$ extension of the Q-scheme of van Leer.

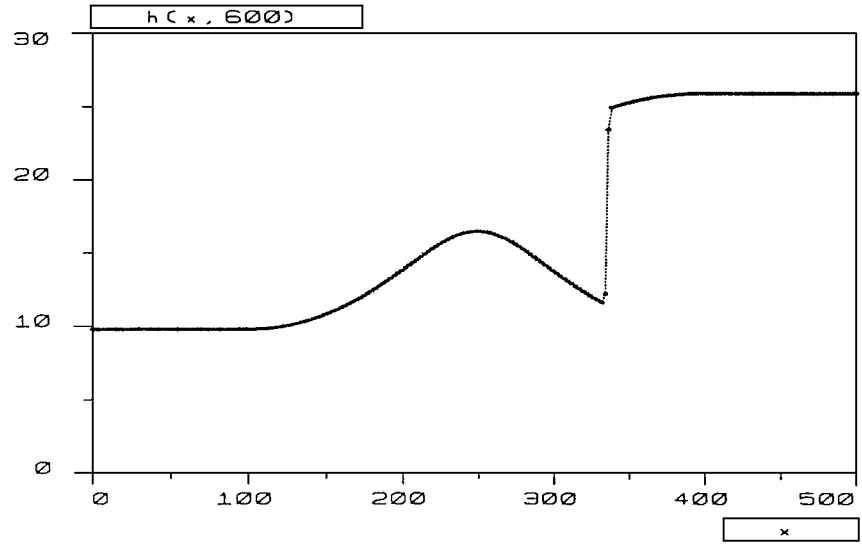

FIG. 28. $h(x, 600)$ extension of the Q-scheme of van Leer.

5.4.2. Surge propagation through converging–diverging channel. This test problem allows us to show the performances of the extensions in a transitory motion and for Froude number greater than the considered in the tidal wave propagation problem.

In this case the exact solution does not exist; then the numerical results are analyzed from a qualitative point of view and can be compared with those presented in [4] with the McCormack TVD scheme.

The time evolution of a surge in the same channel of the previous test is considered. A bore 9.79 m deep of 1000 cum/s propagates downstream over still water 1-m deep. A 2-m weir is supposed to be placed downstream. Also in this case CFL $= 0.9$, M $= 0$, and 200 is the number of nodes.

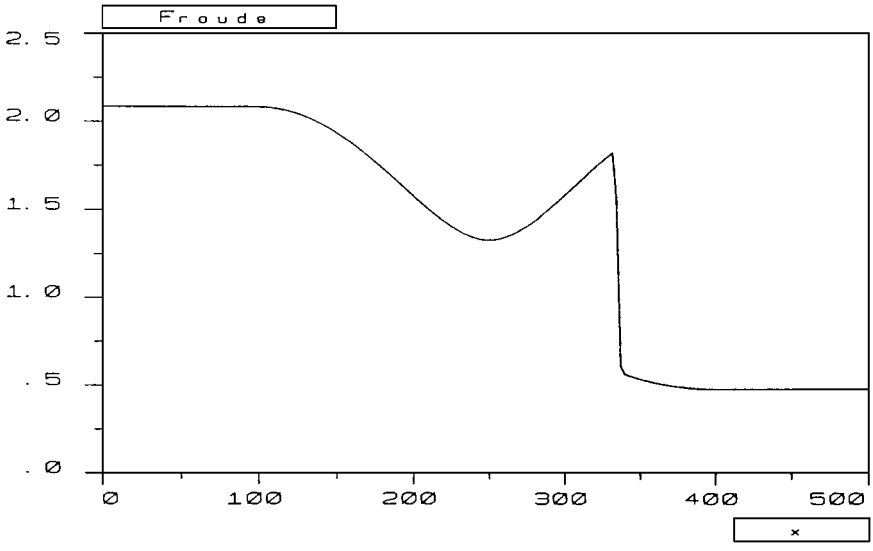

FIG. 29. Froude number $t = 600$.

The situation at $t = 5$ s is plotted in Fig. 25. At this time the weir condition closed the channel and the supercritical front advances through the contracting channel. At time $t = 15$ s (see Fig. 26) the front has surpassed the point of maximum contraction. And time at $t = 150$ s (see Fig. 27) the downstream end is reached by a front similar to the initial one so that is partially reflected and partially transmitted over the weir. The reflected surge starts travelling upstream and it propagates until it becomes a stationary hydraulic jump in the contracting region. This final steady state is shown in Fig. 28 ($t = 600$ s) and the corresponding Froude number is in Fig. 29.

6. CONCLUSIONS

In this this paper the shallow water equations in channels with irregular geometry are solved with extensions of the Q-schemes of van Leer and Roe. The main contribution of this work is an improved discretization of the source terms. The efficiency of the proposed schemes is proved. This analysis is done in terms of a conservation property which is related with a stationary solution also introduced in this paper. This solution allows to test the numerical schemes in subcritical and supercritical cases with variable geometry and taking into account the friction effect. To complete this study an asymptotic unsteady solution for small Froude number is also obtained and the different schemes are compared with this solution. The comparison of the studied schemes with high-order methods like McCormack TVD scheme [4] in relevant test problems with hydraulic jumps and transient motions for large Froude numbers is also satisfactory. Numerical results and theoretical developments now in progress with García-Navarro [5] confirm the importance of upwinding the source terms also in channels of arbitrary cross section.

ACKNOWLEDGMENTS

The author is indebted to A. Bermúdez, P. Gracía-Navarro, and J. Liñares for many valuable discussions. This work has been supported by DGYCIT MAR97-1055-C02-01.

REFERENCES

1. F. Alcrudo and P. García-Navarro, A high-resolution Godunov-type scheme in finite volumes for the 2D shallow-water equations. *Int. J. Numer. Methods Fluids* **16**, 489 (1993).
2. A. Bermúdez, A. Dervieux, J. A. Desideri, and M. E. Vázquez, Upwind schemes for the two-dimensional shallow water equations with variable depth using unstructured meshes, *Comput. Methods Appl. Mech. Eng.* **155**, 49 (1998).
3. A. Bermúdez and M. E. Vázquez, Upwind methods for hyperbolic conservation laws with source terms, *Comput. & Fluids* **23**(8), 1049 (1994).
4. P. García-Navarro, F. Alcrudo, and J. M. Savirón, 1D open channel flow simulation using TVD MacCormack scheme, *J. Hydraulic Eng.* **118**(10), 1359 (1992).
5. P. García-Navarro and M. E. Vázquez-Cendón, *Some Considerations and Improvements on the Performance of Roe's Scheme for 1D Irregular Geometries*, Technical Report 23, Departamento de Matemática Aplicada, Universidad de Santiago de Compostela, 1997. *Comput. & Fluids*, submited.
6. P. Glaister, Approximate Riemann solutions of the shallow water equations, *J. Hydraulic Res*. **26**, 293 (1988).
7. P. Glaister, Prediction of supercritical flow in open channels, *Comput. & Math. Appl.* **24**(7), 69 (1992).
8. E. Godlewski and P. A. Raviart, in *Numerical Approximation of Hyperbolic Systems of Conservation Laws*, of Applied Mathematical Sciences, Vol. 118. (Springer-Verlag, New York, 1996).

9. N. Goutal and F. Maurel, *Proceedings of the 2nd Workshop on Dam-Break Wave Simulation*, Technical Report HE-43/97/016/A, Electricité de France, Département Laboratoire National d'Hydraulique, Groupe Hydraulique Fluviale, 1997.
10. J. M. Greenberg and A. LeRoux, A well-balanced scheme for the numerical processing of source terms in hyperbolic equations, *SIAM J. Numer. Anal.* **33**(1), 1 (1996).
11. A. Harten, On a class of high resolution total-variation-stable finite-difference schemes, *SIAM J. Numer. Anal.* **21**(1), 1 (1984).
12. A. Harten, P. Lax, and A. van Leer, On upstream differencing and Godunov-type schemes for hyperbolic conservation laws, *SIAM Rev.* **25**, 35 (1983).
13. R. LeVeque, *Numerical Methods for Conservation Laws* (Birkhäuser, Basel/Boston/Berlin, 1990).
14. R. LeVeque and H. C. Yee, A study of numerical methods for hyperbolic conservation laws with stiff source terms, *J. Comput. Phys.* **86**, 187 (1990).
15. T.-P. Liu, Quasilinear hyperbolic systems, *Commun. Math. Phys.* **68**, 141 (1979).
16. I. MacDonald, *Tests Problems with Analytic Solutions for Steady Open Channel Flow*, Technical Numer. Anal. Report 6/94, University of Reading, 1994.
17. A. Priestley, *Roe-Type Schemes for Super-critical Flows in Rivers*, Numer. Anal. Report 13/89, Reading University, 1989.
18. P. L. Roe, Approximate Riemann solvers, parameter vectors, and difference schemes, *J. Comput. Phys.* **43**, 357 (1981).
19. P. L. Roe, Upwind differenced schemes for hyperbolic conservation laws with source terms, in *Proceedings of the Conference on Hyperbolic Problems*, edited by Carasso, Raviart, and Serre, p. 41 (Springer-Verlag, New York, 1986).
20. E. F. Toro, *Riemann Solvers and Numerical Methods for Fluid Dynamics. A Practical Introduction* (Springer-Verlag, New York, 1997).
21. B. van Leer, On the relation between the upwind-differencing schemes of Godunov, Engquist-Osher and Roe, *SIAM J. Sci. Statist. Comput.* **5**(1), 1 (1984).
22. M. E. Vázquez-Cendón, Estudio de esquemas descentrados para su aplicación a las leyes de conservación hiperbólicas con términos fuente, Tesis doctoral, Departamento de Matemática Aplicada, Universidad de Santiago de Compostela, Spain, 1994.